Inferring Autonomic Nervous System Stimulation from Hand and Foot Skin Conductance Measurements

Md. Rafiul Amin, *Student Member, IEEE,* Rose T. Faghih, *Member, IEEE*

Abstract— The autonomic nervous system (ANS) stimulates various sweat glands. Changes in skin conductance measurements indicate sudomotor nerve activity (SMNA), and could be used in inferring the underlying ANS stimulation. We model hand and foot skin conductance measurements simultaneously using a state-space model with Gaussian errors and sparse impulsive events as inputs to the model. Using a multi-rate formulation, we recover the timing and amplitudes of SMNA using a generalized cross-validation based sparse recovery approach. We analyze experimental and simulated data to validate the performance of the proposed approach and illustrate that we are able to recover the underlying auditory stimuli.

I. INTRODUCTION

Electrodermal activity (EDA) represents the changes in the electrical properties of skin due to sweating. Hypothalamic areas control sweating primarily for thermoregulation of the body. However, sweat secretion can also occur due to other physiological events including emotional arousal [1]. Moreover, changes in skin conductance (SC), a measure of EDA, are highly correlated with emotions and can be used for interpreting emotional dysregulation and disturbances [2], [3]. Changes in SC throughout the body are controlled by the autonomic nervous system (ANS) [4]. The Analysis of SC time series modulated by the ANS can help monitor the mental health of an individual in order to prevent stress-related health problems [5].

Many researchers have proposed different methods for the deconvolution of SC time series to infer the timings and amplitudes of stimulation as well as to estimate the underlying physiological parameters with the goal of uncovering emotional states using single channel SC data. Benedek *et al.* [6] proposed a non-negative deconvolution scheme from single SC time series to separate them into discrete compact responses. They have also assessed deviations of SC responses from the standard SC response shape. However, their deconvolution scheme could capture noise as SC responses and does not include individual differences in the modeling of the rise and decay times. Greco *et al.* [7] proposed a quadratic programming formulation to decompose SC time series into tonic and phasic components. In their formulation, they considered the sparsity condition in neural stimuli from the ANS. However, the use of a fixed regularization parameter for imposing the sparsity constraint makes it challenging to find an accurate sparse solution. In

Md. Rafiul Amin and Rose T. Faghih are with the Computational Medicine Lab in the Department of Electrical and Computer Engineering, University of Houston, Houston, TX, 77204-4005 USA e-mail: mamin@uh.edu, rtfaghih@uh.edu

another work, Gallego *et al.* [8] proposed a decomposition approach to obtain a sparser solution in less time; however, this approach leads to overly sparse solutions compared to the underlying neural stimuli. Faghih *et al.* [9], [10], [11], [12] proposed a two-step coordinate descent deconvolution approach to account for individual differences in the physiological system parameters. However, inferring the ANS stimulation as well as physiological system parameters using only one channel of SC data is challenging in presence of noise.

Extensive research has been conducted to collect EDA using wearable sensors that can provide better insight into how affect and stress interact with daily life [13], [14], [15]. Nevertheless, wearable sensors often suffer from poor signal acquisition and motion artifacts. Moreover, adequate analysis of EDA data in presence of artifacts and noise is yet to be undertaken. Incorporating multiple channel data with wearables to account for the poor signal acquisition could potentially improve the deconvolution result. Faghih *et al.* [16] proposed an approach to include both of the cortisol and Adrenocorticotropic hormone (ACTH) time series using a single state-space model, and then, they formulated a concurrent deconvolution scheme of these hormone data.

Inspired by the work by Faghih *et al.* [16] for concurrent deconvolution of the cortisol and ACTH hormone time series, we utilize concurrently collected hand and foot skin conductance measurements to robustly infer the ANS stimulation. We hypothesize that the changes in SC in different parts of the body are due to the same ANS stimulation. We propose a state-space model that includes the SC measurements from the volar surfaces of both hand and foot. Moreover, we propose a concurrent deconvolution algorithm and analyze SC data using auditory stimulation experimental data.

II. METHODS

A. Dataset Description

We used the SC responses to loud sounds, simultaneously recorded from palm, fingers and foot data [17], which was collected for modeling event-related SC responses. The dataset contains SC data recorded from 3 different locations (the hypothenar of the non-dominant hand, the middle phalanx of the dominant second and third finger and the medial plantar surface of the non-dominant foot) of each of the 26 healthy participants in response to 20 auditory stimuli (each of them is single white noise bursts of 1s duration). Participants were asked to press a foot operated pedal upon hearing the stimuli. A detailed description of the experiment is given in [18]. We use simultaneous SC recordings from
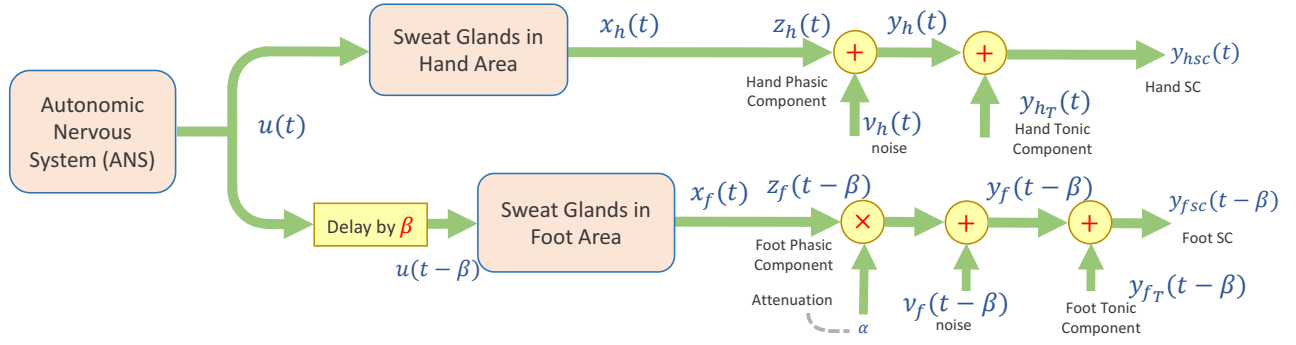
Fig. 1: **System Model Block Diagram.** A single neural stimuli signal $u(t)$ generated by the ANS is responsible for the phasic response in different regions of the skin throughout the body. The block diagram shows the same neural stimuli $u(t)$ is stimulating two different regions with a delay β. The attenuation term α reflects the ratio of the number of sweat glands in the foot region to that of the hand region.

the middle phalanx of the dominant second and third finger and the medial plantar surface of the non-dominant foot for our study. Throughout the paper, we name them as hand SC data and foot SC data, respectively. We discarded the data corrupted with heavy noise or artifacts and the data having very small SC responses.

B. Model Formulation for Phasic SC Deconvolution

The changes in SC, caused by eccrine sweat glands activity, are stimulated by sudomotor nerve activity (SMNA) in the ANS. SC data can be represented as the summation of a fast varying component and a slowly varying component. The slowly varying component of SC data, known as the tonic component, is mainly intended for thermoregulation of the body and the comparatively fast varying component, designated as the phasic component, represents the activity of ANS which is a reflection of emotional events. The SC signal can be written as the summation of these two components as follows:

$$y_{sc}(t) = y(t) + y_T(t)$$

where $y_{sc}(t)$, $y(t)$ and $y_T(t)$ represent the measured SC signal, phasic component and tonic component, respectively. Throughout the paper, $y_{hsc}(t)$, $y_h(t)$ and $y_{h_T}(t)$ correspond respectively to the SC signal, phasic component and tonic component from hand and $y_{fsc}(t)$, $y_f(t)$ and $y_{f_T}(t)$ correspond to the SC signal, phasic component and tonic component from the foot, respectively. In the preprocessing stage, we remove the tonic components $y_{h_T}(t)$ and $y_{f_T}(t)$ from the SC data $y_{hsc}(t)$ and $y_{fsc}(t)$ using the cvxEDA algorithm [7] and separate out the phasic components $y_h(t)$ and $y_f(t)$ for hand and foot, respectively. In this case, we use the default value of the regularization parameter for l_1-norm minimization. We assume that the extracted phasic components have some Gaussian noise added which we consider as the measurement noise for them. We hypothesize that the same ANS stimulation modulates the phasic component of SC data in different eccrine sweat glands of the human body. We propose a state-space model with hand and foot phasic SC data and the ANS input. Figure 1 shows the complete block diagram of the proposed system modeling. The state-space model is as follows:

$$\tau_r \tau_d \frac{d^2 x_h(t)}{dt^2} + (\tau_r + \tau_d)\frac{dx_h(t)}{dt} + x_h(t) = u(t) \quad (1)$$

$$\tau_r \tau_d \frac{d^2 x_f(t)}{dt^2} + (\tau_r + \tau_d)\frac{dx_f(t)}{dt} + x_f(t) = u(t - \beta) \quad (2)$$

where $x_h(t)$ and $x_f(t)$ are the two internal states which are reflected into the observed phasic components from the hand and foot, respectively. α refers to an attenuation term which is related to the ratio of the number of sweat glands in both the hand and foot. The term β refers to the delay in the foot stimuli input and τ_r and τ_d are the rise and decay times of the SC responses, respectively. β can be calculated by taking the cross-correlation of the hand and foot phasic SC data before deconvolution. The locations of the maximum values of the cross-correlations of the hand and foot SC signal are used to calculate the time lags β. Under the assumption that the ANS stimuli are sparse as in [12], we represent the input as $u(t) = \sum_{i=1}^{N} q_i \delta(t - \Delta_i)$ where q_i is the amplitude of the impulse in the neural stimuli at time Δ_i. Let T_u be the sampling frequency of the neural stimuli and T_y be the sampling frequency of the phasic SC data for each channel. Timings of the neural impulses can be written as $\Delta_i = iT_u$. q_i is zero if there is no impulse in the stimuli. Let y_{h_k} and y_{f_k} be the observed phasic SC from the hand and foot respectively at time instance $t_k = kT_y$.

$$y_{h_k} = z_h(t_k) + v_{h_k} \quad (3)$$
$$y_{f_k} = \alpha z_f(t_k) + v_{f_k} \quad (4)$$

where $z_h(t) = x_h(t)$ and $z_f(t) = x_f(t + \beta)$. v_{h_k} and v_{f_k} represent the measurement noise in each channel and we model them as zero-mean Gaussian random variables. These are the sampled values from the measurement noise continuous variables $v_h(t)$ and $v_f(t)$, respectively. Let $x_1(t)$ and $x_3(t)$ be two internal states, $x_2(t) = z_h(t)$, and $x_4(t) = z_f(t)$. Also, let the phasic SC measurement $y_1(t) = y_h(t)$ and $y_2(t) = y_f(t)$ and measurement noise $v_1(t) = v_h(t)$ and $v_2(t) = v_f(t)$. We can write the system equations in (1)-(4) in a state-space

form as follows:

$$\dot{x}(t) = \mathscr{A}_c x(t) + \mathscr{B}_c u(t)$$
$$y(t) = \mathscr{C}_c x(t) + v(t).$$

where $x(t) = \begin{bmatrix} x_1(t) \\ x_2(t) \\ x_3(t) \\ x_4(t) \end{bmatrix}$, $y(t) = \begin{bmatrix} y_1(t) \\ y_2(t) \end{bmatrix}$, $v(t) = \begin{bmatrix} v_1(t) \\ v_2(t) \end{bmatrix}$

$\mathscr{A}_c = \begin{bmatrix} -\frac{1}{\tau_r} & 0 & 0 & 0 \\ \frac{1}{\tau_d} & -\frac{1}{\tau_d} & 0 & 0 \\ 0 & 0 & -\frac{1}{\tau_r} & 0 \\ 0 & 0 & \frac{1}{\tau_d} & -\frac{1}{\tau_d} \end{bmatrix}$, $\mathscr{B}_c = \begin{bmatrix} 1/\tau_r \\ 0 \\ 1/\tau_r \\ 0 \end{bmatrix}$ and $\mathscr{C}_c = \begin{bmatrix} 0 & 1 & 0 & 0 \\ 0 & 0 & 0 & \alpha \end{bmatrix}$.

We derive the discrete analog of the system assuming that the input and the states are constant over T_u and the discrete version of the neural stimuli can be written as a vector $u = [q_1 \ q_2 \ \cdots \ q_N]^\top$ that represents the entire neural stimuli over the duration of SC data. Let $\Phi = e^{AT_u}$, and $\Gamma = \int_0^{T_u} e^{A(T_u - \rho)} d\rho$ to write the discrete state-space form as:

$$x[k+1] = \Phi x[k] + \Gamma u[k]$$
$$y[k] = \mathscr{C}_c x[k] + v[k].$$

As neural stimuli and SC measurement have different sampling frequencies, i.e. $T_y = LT_u$ (L is a positive integer), we let $\mathscr{A}_d = \Phi^L$, $\mathscr{B}_d = \begin{bmatrix} \Phi^{L-1}\Gamma & \Phi^{L-2}\Gamma & \cdots & \Gamma \end{bmatrix}$, $u_d[k] = \begin{bmatrix} u[Lk] & u[Lk+1] & \cdots & u[Lk+L-1] \end{bmatrix}^\top$, $v_d[k] = v[Lk]$ and $x_d[k] = x_d[Lk]$; the multi-rate system can be represented as follows:

$$x_d[k+1] = \mathscr{A}_d x_d[k] + \mathscr{B}_d u_d[k] \quad (5)$$
$$y[k] = \mathscr{C}_c x_d[k] + v_d[k] \quad (6)$$

where $\mathscr{A}_d$ and $\mathscr{B}_d$ are functions of $\tau = \begin{bmatrix} \tau_r & \tau_d \end{bmatrix}^\top$, α, T_u and T_y. Let $\theta = \begin{bmatrix} \tau^\top & \alpha \end{bmatrix}^\top$. As the system is causal, we use (5)-(6) to obtain the observation equation for kth sample:

$$y[k] = \mathscr{F}[k] x_d[0] + \mathscr{D}[k] \mathbf{u} + v_d[k]$$

where $\mathscr{F}[k] = \mathscr{C}_c \mathscr{A}_d^k$, $\mathscr{D}[k] = \mathscr{C}_c \begin{bmatrix} \mathscr{A}_d^{k-1}\mathscr{B}_d & \mathscr{A}_d^{k-2}\mathscr{B}_d & \cdots & \mathscr{B}_d & \underbrace{0 \ \cdots \ 0}_{N-kL} \end{bmatrix}$, and $\mathbf{u} = \begin{bmatrix} u_d[0] & u_d[1] & \cdots & u_d[k-1] & \cdots & u_d[M-1] \end{bmatrix}^\top_{N \times 1}$. For the initial condition, we can let $y_0 = x_d[0] = \begin{bmatrix} 0 & y_h(0) & 0 & \frac{y_f(0)}{\alpha} \end{bmatrix}^\top$ similar to the work in [12]. Then, let $\mathbf{y} = \begin{bmatrix} y[1]^\top & y[2]^\top & \cdots & y[M]^\top \end{bmatrix}^\top_{2M \times 1}$, where $y[k] = \begin{bmatrix} y_{h_k} & y_{f_k} \end{bmatrix}^\top$ for all $k = 1, 2 \cdots, M$. Moreover, let $\mathscr{F}_\theta = \begin{bmatrix} \mathscr{F}[0] & \mathscr{F}[1] & \cdots & \mathscr{F}[M-1] \end{bmatrix}^\top_{2M \times 4}$, $\mathscr{D}_\theta = \begin{bmatrix} \mathscr{D}[0] & \mathscr{D}[1] & \cdots & \mathscr{D}[M-1] \end{bmatrix}^\top_{2M \times N}$, and $v = \begin{bmatrix} v[1] & v[2] & \cdots & v[M] \end{bmatrix}^\top_{2M \times 1}$. Therefore, we can write the observation equation for all the sampled data as follows:

$$\mathbf{y} = \mathscr{F}_\theta y_0 + \mathscr{D}_\theta \mathbf{u} + v.$$

Equivalently, we can represent the system as:

$$\mathbf{y}_h = \mathscr{F}_{\theta_h} y_0 + \mathscr{D}_{\theta_h} \mathbf{u} + v_h \quad (7)$$
$$\mathbf{y}_f = \mathscr{F}_{\theta_f} y_0 + \mathscr{D}_{\theta_f} \mathbf{u} + v_f. \quad (8)$$

Here $\mathbf{y}_h$, $\mathscr{F}_{\theta_h}$, $\mathscr{D}_{\theta_h}$, and v_h correspond to the odd rows of $\mathbf{y}$, $\mathscr{F}_\theta$, $\mathscr{D}_\theta$, and v, respectively, and $\mathbf{y}_f$, $\mathscr{F}_{\theta_f}$, $\mathscr{D}_{\theta_f}$, and v_f correspond to the even rows of $\mathbf{y}$, $\mathscr{F}_\theta$, $\mathscr{D}_\theta$, and v, respectively.

Noise Variance Estimation: According to our assumption, the noise is a Gaussian random variable with zero mean and non zero variance. The spectral energy of the noise is distributed over the whole spectral range of 0 to half of the sampling frequency. For experimental SC signal, we filter the phasic component of the SC signal with a 0.5 Hz high pass filter. Then, we take the variance of the signal to obtain an estimate of the noise variance in the high-frequency region assuming the SC phasic responses does not exist in the high-frequency region beyond 0.5 Hz. We interpolate this calculated noise for the whole bandwidth including the low-frequency region. This allows us to obtain an estimate of the ratio of the noise variances σ_h^2 and σ_f^2 of hand and foot phasic SC data, respectively.

C. Estimation

The sampling interval for phasic SC data and neural stimuli is $T_y = 1$ seconds $T_u = 0.25$ seconds, respectively. In order to estimate the system parameters and the neural stimuli, we use (7)-(8), and formulate the following optimization problem assuming the sparsity constraint on $\mathbf{u}$:

$$\underset{\substack{\tau, \alpha, \mathbf{u}, \lambda \\ 0.1 \leq \tau_r \leq 1.4, \ 1.5 \leq \tau_d \leq 6 \\ 0.01 \leq \alpha \leq 1 \mathbf{u} \geq 0, 0 \leq \lambda \leq 0.1}}{\operatorname{argmin}} \quad J(\theta, \mathbf{u}, \lambda) = \frac{1}{2\sigma_h^2} ||\mathbf{y}_h - \mathscr{F}_{\theta_h} y_0 - \mathscr{D}_{\theta_h} \mathbf{u}||_2^2$$

$$+ \frac{1}{2\sigma_f^2} ||\mathbf{y}_f - \mathscr{F}_{\theta_f} y_0 - \mathscr{D}_{\theta_f} \mathbf{u}||_2^2 + \lambda ||\mathbf{u}||_p^p \quad (9)$$

Here, the l_p-norm is an approximation of the l_0-norm ($0 < p \leq 2$) and the l_p-norm regularization parameter λ is chosen such that there is a balance between filtering out the noise and the sparsity level of $\mathbf{u}$. We can solve the inverse problem of finding a nonnegative $\mathbf{u}$ with a specific sparsity level using the Focal Underdetermined System Solver (FOCUSS+) algorithm [19]. To calculate an appropriate value of the l_p-norm regularization parameter λ adaptively, we use the generalized crossvalidation (GCV) technique similar to the approach in [16], [10], [12]. We use the singular value decomposition based GCV technique by Zdunek *et al.* [20] for estimating λ by minimizing:

$$\underset{\substack{\lambda \\ 0 \leq \lambda \leq 0.1}}{\operatorname{argmin}} \ G(\lambda | \theta, \mathbf{u}) = \frac{\left[\mathscr{L} \sum_{i=1}^{\mathscr{L}} \gamma_i^2 \left(\frac{\lambda}{\kappa_i^2 + \lambda} \right)^2 \right]}{\left[\sum_{i=1}^{\mathscr{L}} \left(\frac{\lambda}{\kappa_i^2 + \lambda} \right)^2 \right]} \quad (10)$$

where $\gamma = \mathbf{R}^\top \mathbf{y}_\theta = \begin{bmatrix} \gamma_1 & \gamma_2 & \cdots & \gamma_{\mathscr{L}} \end{bmatrix}^\top$ with $\mathbf{y}_\theta = \mathbf{y} - \mathscr{D}_\theta y_0$, and $\mathscr{D}_\theta \mathbf{P_u}^{\frac{1}{2}} = \mathbf{R} \Sigma \mathbf{Q}^\top$ with $\mathbf{P_u} = \operatorname{diag}(|u_i|^{2-p})$ and $\Sigma = \operatorname{diag}\{\kappa_i\}$; $\mathbf{R}$ and $\mathbf{Q}$ are unitary matrices and the κ_i's are the singular values of $\mathscr{D}_\theta \mathbf{P_u}^{\frac{1}{2}}$; $\mathscr{L}$ is the total number of data points in $\mathbf{y}_h$ and $\mathbf{y}_f$, i.e., $\mathscr{L} = 2M$ [20].

We solve the optimization problem in (9) using the following algorithm:

Algorithm: Concurrent Deconvolution

(a) Let i = 0.

Initialization:

(b) Initialize $\tilde{\theta}^0$ by sampling a uniform random variable on $\begin{bmatrix} 0.10 & 1.4 \end{bmatrix}$ for $\tilde{\tau}_r^{(0)}$, on $\begin{bmatrix} 1.5 & 6 \end{bmatrix}$ for $\tilde{\tau}_d^{(0)}$, and on $\begin{bmatrix} 0.01 & 1 \end{bmatrix}$ for $\tilde{\alpha}^0$; let $j = 1$.

(c) Set $\theta = \tilde{\theta}^{(j-1)}$; use FOCUSS+ to solve the inverse problem in (9) to find the stimuli $\tilde{\mathbf{u}}^{(j)}$ by initializing $\tilde{\mathbf{u}}^{(0)}$ at a vector with all ones.

(d) Set $\mathbf{u} = \tilde{\mathbf{u}}^{(j)}$; use the interior point method and minimize the optimization problem in (9) to solve for $\tilde{\theta}^{(j)}$. Let $j = j+1$.

(e) Repeat between steps (c)-(d) until $j = 30$.

(f) Set $\hat{\theta}^0 = \tilde{\theta}^{(j)}$ and $\hat{\mathbf{u}}^0 = \tilde{\mathbf{u}}^{(j)}$.

Outer Optimization Problem:

(g) Set $i = i+1$.

(h) Set $\theta = \hat{\theta}^{(i-1)}$; obtain $\hat{\mathbf{u}}^{(i)}$ solving the following steps:

  i. Set $m = 0$ and $\hat{\mathbf{u}}^{(i)^{(0)}} = \hat{\mathbf{u}}^{(i)}$ and $\hat{\lambda}^{(i)^{(0)}} = 2 \times 10^{-3}$.
    Inner Optimization Problem:

  ii. Set $m = m+1$.

  iii. Set $\lambda = \hat{\lambda}^{(i)^{(m-1)}}$ and $\theta = \hat{\theta}^{(i-1)}$; solve for $\hat{\mathbf{u}}^{(i)^{(m)}}$ by initializing the optimization problem in (9) at $\mathbf{u} = \hat{\mathbf{u}}^{(i)^{(m-1)}}$.

  iv. Set $\mathbf{u} = \hat{\mathbf{u}}^{(i)^{(m-1)}}$ and $\theta = \hat{\theta}^{(i-1)}$; solve for $\lambda^{(i)^{(m)}}$ by initializing the optimization problem in (10) at $\lambda = \hat{\lambda}^{(i)^{(m-1)}}$.

  v. repeat (ii)-(iv) until convergence and set $\hat{\mathbf{u}}^{(i)} = \hat{\mathbf{u}}^{(i)^{(m)}}$.

(i) Set $\mathbf{u}$ equal to $\hat{\mathbf{u}}^{(i)}$; solve for $\hat{\theta}^{(i)}$ using interior-point method by initializing the optimization problem in (9) at $\hat{\theta}^{(i-1)}$.

(j) Iterate between (g)-(i) until convergence.

We start with several random initial values for system parameters and run the algorithm. Finally, we choose the best estimate that has the minimum value for the cost function in (9).

III. RESULTS

Using the proposed approach, we concurrently deconvolve hand and foot SC measurements collected during an auditory stimulation experiment and recover the underlying stimuli $u(t)$ and the corresponding rise time (τ_r) and decay times (τ_d) of SC responses as well as the foot attenuation (α). Results in Figure 2 show that the proposed algorithm successfully recovers the timings and amplitudes of neural stimuli as well as the underlying system parameters, i.e. the rise and decay times for two female participants (subject ID: 15 and 12) and

TABLE I: Deconvolution Errors with Our Single Channel and Concurrent Deconvolution using Simulated Data

Approaches	$\frac{\sum \lvert \Delta_i - \hat{\Delta}_i \rvert}{\lVert \hat{\mathbf{u}} \rVert_0}$	$\frac{\lVert \mathbf{u} - \hat{\mathbf{u}} \rVert}{\lVert \mathbf{u} \rVert_0}$	$\frac{\lvert \tau_1 - \hat{\tau}_1 \rvert}{\tau_1} \times 100\%$	$\frac{\lvert \tau_2 - \hat{\tau}_2 \rvert}{\tau_2} \times 100\%$
Only Hand	0.26	0.61	5.80	8.25
Only Foot	0.28	1.22	21.57	6.83
Concurrent	0.18	0.46	1.23	3.26

Symbols with hat and without hat denote the estimated values and the true values of the parameters, respectively.

two male participants (subject ID: 11 and 26). We considered the signal segment from 200 seconds to 400 seconds for our analysis. The multiple correlation coefficient (R^2) has been calculated for all the four reconstructed signals. The high values of R^2 (found to be greater than 0.97 for hand) for hand phasic SC data suggest that our proposed algorithm can successfully uncover underlying physiologically plausible ANS stimulation. For foot data, the R^2 values are greater than 0.90. Lower R^2 values for foot data suggest that foot datasets are noisier than the hand datasets.

The estimated delay between hand and foot phasic SC data (denoted by β) for the two female and two male subjects are 1.47 seconds, 1.12 seconds, 1.15 seconds and 1.43 seconds, respectively. The estimated mean delays from auditory stimulations to hand phasic SC data are 2.14 seconds, 1.80 seconds, 1.70 seconds and 1.70 seconds, respectively. The recovered attenuation parameters α, i.e. the attenuation in foot SC data compared to hand SC data are 0.0736, 0.4028, 0.3635 and 0.4121, respectively. Rise times τ_r are 0.56, 0.79, 0.77 and 0.52 seconds and decay times τ_d are 3.10, 3.12, 3.02 and 2.89 seconds, respectively.

To further validate our approach, we simulated noisy data using the model parameters $\tau_r = 0.75$, $\tau_d = 4$ and $\alpha = 0.3$ and a synthetic input. In this case, we have the ground truth for comparison. To simulate noisy data, we added zero-mean Gaussian noise with 20 dB and 15 dB SNR to the hand and foot phasic SC data, respectively. These two levels of noise are chosen given the higher levels of noise in foot data. Figure 3 shows the simulated data for both channels. We perform deconvolution on the simulated noisy data. Figure 3 also shows the deconvolution performance of other existing algorithms for comparison as well as our single channel deconvolution approach. Results using simulated data show our concurrent deconvolution scheme is outperforming existing methods. The last three panels in Figure 3 and the corresponding estimation errors in Table I show our concurrent deconvolution is performing better than our single channel deconvolution results.

IV. DISCUSSIONS

Deconvolution of SC data is a challenging problem. There can exist multiple sets of physiological parameters and stimuli that closely approximate an observed signal. In addition, the smallest level of noise can perturb the solution to a physiologically infeasible point due to the sensitive nature of the bi-exponential function. We formulate a non-convex problem and solve it using a coordinate descent deconvolution approach until convergence to a local
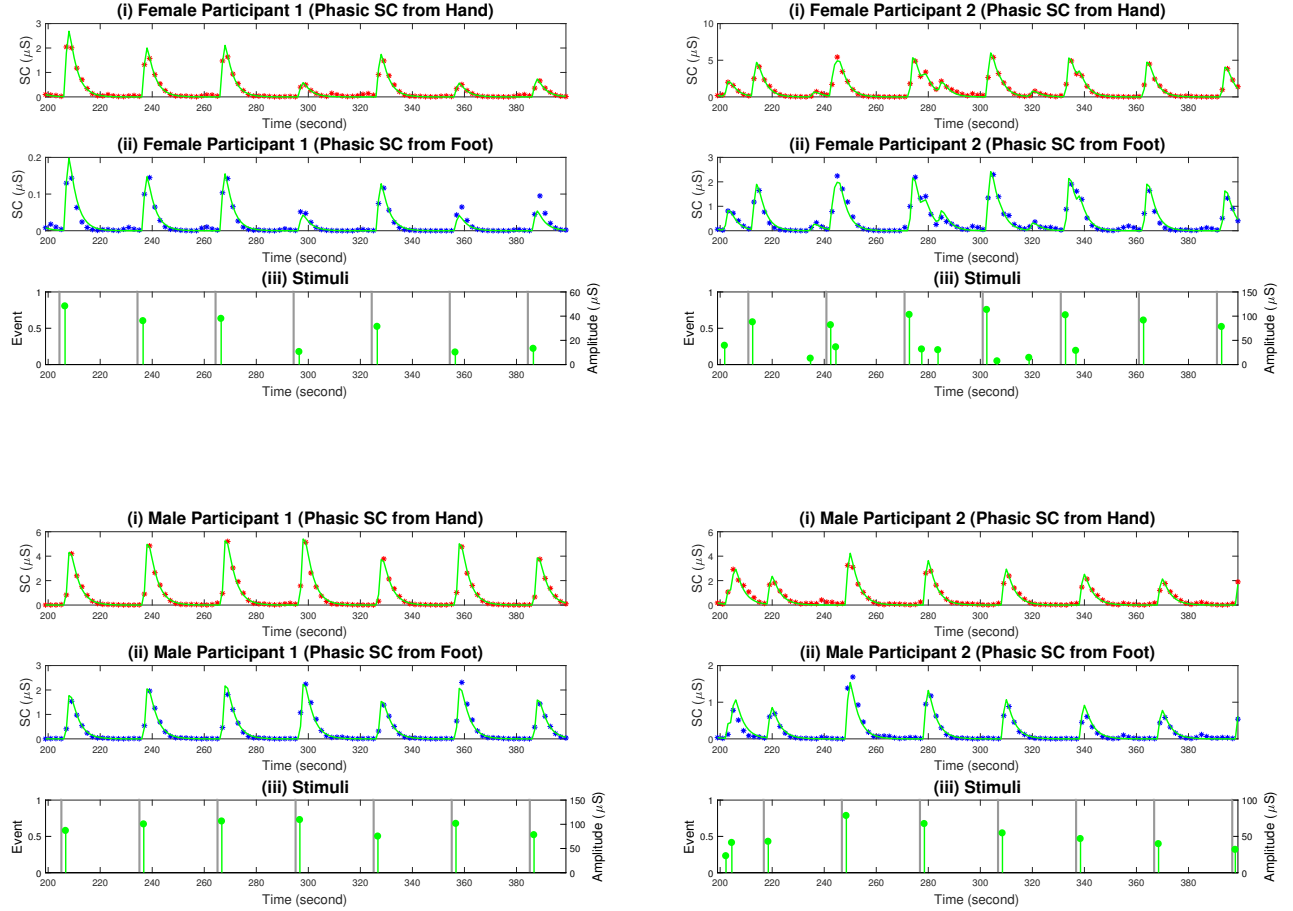
Fig. 2: **Estimated Deconvolution of the Experimental Phasic SC Signals Two Female and Two Male Particiapants:** In each of the panels, i) the top sub-panel shows the experimental (red stars) and the estimated (green curve) hand phasic component; ii) middle sub-panel shows the experimental (blue stars) and estimated (green curve) foot phasic component; and iii) bottom sub-panel shows the timings of the auditory stimuli (gray vertical lines) and the estimated ANS activation timings and amplitudes (green vertical lines).

minimum. We use multiple initializations, and choose the solution that minimizes the cost function compared to all other solutions that the algorithm finds. To make sure the problem is identifiable, we use appropriate constraints on the unknowns to obtain physiologically plausible solutions. Figure 3 shows the performance of LedaLab [6] and cvxEDA [7]. These two existing methods can only solve the inverse problem of finding **u** using single channel data assuming known physiological parameters. In contrast, the proposed approach can solve for both the physiological parameters and the inverse problem using multichannel data.

According to our investigation with the analyzed auditory stimulation data, usually, there is a very large phasic response right after a stimulation has been given to the subject. In case of female participant 2, the SC data shows multiple responses after one auditory stimulation. Our algorithm successfully detected these small responses. Generally, the distance between two consecutive phasic responses is more than a few seconds. Therefore, we chose a minimum separation of 1

second between two adjacent peaks in the deconvolution algorithm.

V. CONCLUSION

In this study, we proposed a physiological state-space model for multiple SC measurements from different locations of the body. Then, we provided a concurrent deconvolution algorithm for multiple simultaneously collected SC data. Analyzing experimental data, we showed our algorithm successfully recovers the neural stimuli due to the known auditory stimulation times. Our approach results in integrating multiple simultaneously collected SC data to recover the ANS stimuli robustly in the presence of noise and different artifacts. The state-space model formulation and deconvolution algorithm successfully recover the stimuli. One of the future directions is to use an inference framework to obtain confidence intervals and reduce the time complexity by avoiding large matrix inversions. Moreover, we can apply an Expectation Maximization approach similar to the one
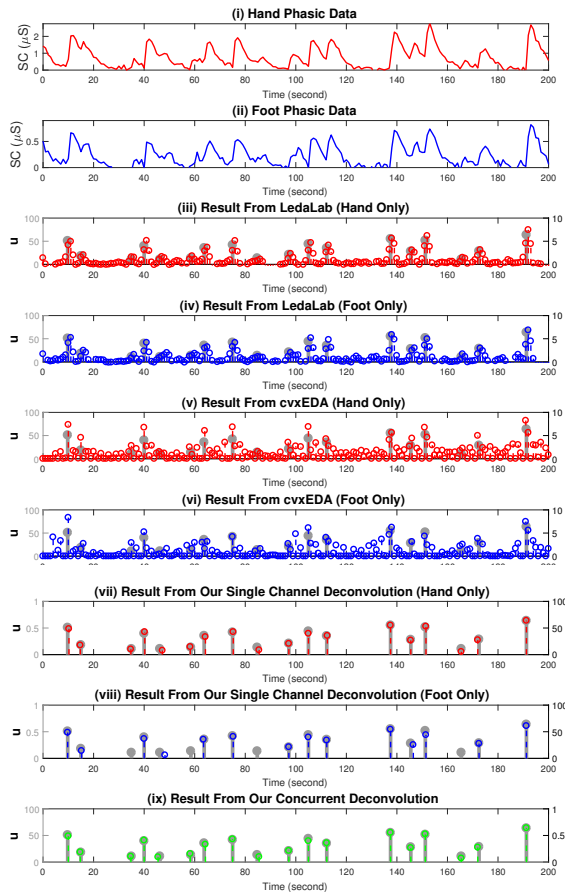
Fig. 3: **Performance Comparison of Proposed Concurrent Deconvolution Approach with Existing Approaches:** The panels (i) and (ii) respectively depict the synthetic simulated data with 20 dB and 15 dB noise for hand and foot. The panels (iii) and (iv) show results with LedaLab [6]. The panels (v) and (vi) show the results with cvxEDA [7]. The panels (vii) and (viii) show the recovered neural stimuli with our single channel deconvolution. The panel (vii) shows the recovered results with our concurrent deconvolution with simulated hand and foot SC data. Gray vertical lines correspond to the ground truth, and red, blue and green vertical lines corresponds to recovered neural stimuli with hand data, foot data and concurrent deconvolution.

proposed by Wickramasuriya *et al.* [21] on the obtained neural stimuli to detect stress.

REFERENCES

[1] J. L. Andreassi, *Psychophysiology: Human behavior & physiological response*. Psychology Press, 2013.

[2] M. E. Dawson, A. M. Schell, and D. L. Filion, "The electrodermal system," *Handbook of psychophysiology*, vol. 2, pp. 200–223, 2007.

[3] H. D. Critchley, "Electrodermal responses: what happens in the brain," *The Neuroscientist*, vol. 8, no. 2, pp. 132–142, 2002.

[4] D. C. Fowles, M. J. Christie, R. Edelberg, W. W. Grings, D. T. Lykken, and P. H. Venables, "Publication recommendations for electrodermal measurements," *Psychophysiology*, vol. 18, no. 3, pp. 232–239, 1981.

[5] J. Wijsman, B. Grundlehner, H. Liu, H. Hermens, and J. Penders, "Towards mental stress detection using wearable physiological sensors," in *Engineering in Medicine and Biology Society, EMBC, 2011 Annual International Conference of the IEEE*. IEEE, 2011, pp. 1798–1801.

[6] M. Benedek and C. Kaernbach, "Decomposition of skin conductance data by means of nonnegative deconvolution," *Psychophysiology*, vol. 47, no. 4, pp. 647–658, 2010.

[7] A. Greco, G. Valenza, A. Lanata, E. P. Scilingo, and L. Citi, "cvxeda: A convex optimization approach to electrodermal activity processing," *IEEE Transactions on Biomedical Engineering*, vol. 63, no. 4, pp. 797–804, 2016.

[8] F. Hernando-Gallego, D. Luengo, and A. Artés-Rodríguez, "Feature extraction of galvanic skin responses by non-negative sparse deconvolution," *IEEE Journal of Biomedical and Health Informatics*, 2017.

[9] R. T. Faghih, "System identification of cortisol secretion: Characterizing pulsatile dynamics," Ph.D. dissertation, Massachusetts Institute of Technology, 2014.

[10] R. T. Faghih, M. A. Dahleh, G. K. Adler, E. B. Klerman, and E. N. Brown, "Deconvolution of serum cortisol levels by using compressed sensing," *PloS one*, vol. 9, no. 1, p. e85204, 2014.

[11] R. T. Faghih, "From physiological signals to pulsatile dynamics: a sparse system identification approach," in *Dynamic Neuroscience*. Springer, 2018, pp. 239–265.

[12] R. T. Faghih, P. A. Stokes, M.-F. Marin, R. G. Zsido, S. Zorowitz, B. L. Rosenbaum, H. Song, M. R. Milad, D. D. Dougherty, E. N. Eskandar *et al.*, "Characterization of fear conditioning and fear extinction by analysis of electrodermal activity," in *Engineering in Medicine and Biology Society (EMBC), 2015 37th Annual International Conference of the IEEE*. IEEE, 2015, pp. 7814–7818.

[13] A. Sano, A. J. Phillips, Z. Y. Amy, A. W. McHill, S. Taylor, N. Jaques, C. A. Czeisler, E. B. Klerman, and R. W. Picard, "Recognizing academic performance, sleep quality, stress level, and mental health using personality traits, wearable sensors and mobile phones," in *Wearable and Implantable Body Sensor Networks (BSN), 2015 IEEE 12th International Conference on*. IEEE, 2015, pp. 1–6.

[14] A. Sano, S. Taylor, A. W. McHill, A. J. Phillips, L. K. Barger, E. Klerman, and R. Picard, "Identifying objective physiological markers and modifiable behaviors for self-reported stress and mental health status using wearable sensors and mobile phones: Observational study," *Journal of medical Internet research*, vol. 20, no. 6, p. e210, 2018.

[15] A. Ghandeharioun, S. Fedor, L. Sangermano, D. Ionescu, J. Alpert, C. Dale, D. Sontag, and R. Picard, "Objective assessment of depressive symptoms with machine learning and wearable sensors data," in *Affective Computing and Intelligent Interaction (ACII), 2017 Seventh International Conference on*. IEEE, 2017, pp. 325–332.

[16] R. T. Faghih, M. A. Dahleh, G. K. Adler, E. B. Klerman, and E. N. Brown, "Quantifying pituitary-adrenal dynamics and deconvolution of concurrent cortisol and adrenocorticotropic hormone data by compressed sensing," *IEEE Transactions on Biomedical Engineering*, vol. 62, no. 10, pp. 2379–2388, 2015.

[17] D. R. Bach, G. Flandin, K. J. Friston, and R. J. Dolan, "PsPM-SCRV10: Skin conductance responses to loud sounds, simultanously recorded from palm, fingers and foot," Feb. 2017. [Online]. Available: https://doi.org/10.5281/zenodo.291465

[18] D. R. Bach, G. Flandin, K. J. Friston, and R. J. Dolan, "Modelling event-related skin conductance responses," *International Journal of Psychophysiology*, vol. 75, no. 3, pp. 349–356, 2010.

[19] J. F. Murray, "Visual recognition, inference and coding using learned sparse overcomplete representations," Ph.D. dissertation, University of California, San Diego, 2005.

[20] R. Zdunek and A. Cichocki, "Improved m-focuss algorithm with overlapping blocks for locally smooth sparse signals," *IEEE Transactions on Signal Processing*, vol. 56, no. 10, pp. 4752–4761, 2008.

[21] D. Wickramasuriya, C. Qi, and R. T. Faghih, "A state-space approach for detecting stress from electrodermal activity," in *Engineering in Medicine and Biology Society (EMBC), 2018 40th Annual International Conference of the IEEE*. IEEE, 2018.